NUMERICAL STUDY OF LAMINAR FLOW IN A SUDDEN EXPANSION OBSTACLED CHANNEL

by

Khudheyer S. MUSHATET[a*], Qais A. RISHAK[b], and Mohsen H. FAGR[c]

[a] College of Engineering, Thi-qar University, Thi-qar, Iraq
[b] Department of Material, College of Engineering, Basra University, Basra, Iraq
[c] Department of Mechanical Engineering, College of Engineering, Thi-qar University, Thi-qar, Iraq

Original scientific paper
DOI: 10.2298/TSCI121029105M

In the present paper, a numerical study has been conducted to investigate the flow heat transfer through an obstacled sudden expansion channel. Rectangular adiabatic obstacles mounted behind the expansion region on the upper and lower wall of the channel used. The effects of obstacles length, obstacles thickness, and number of obstacles on flow and thermal fields for different Reynolds number and expansion ratio examined. Three values of expansion ratio equal to 1.5, 1.75, and 2 were used. The choice of values of Reynolds number takes in consideration the symmetry state. The governing equations of continuity, momentum, and energy discretized by using the finite difference formulation and the resulting algebraic equations solved by using Gauss-Seidle iteration method. The obtained results show that the obstacles have a considerable effect on dynamics of the flow and enhancement of heat transfer. In addition, it is found that the heat transfer is enhanced more as the obstacles thickness increases and this trend is decreased as the obstacles length increases.

Key words: *sudden expansion channel, laminar flow, obstacles*

Introduction

The sudden enlargement channels are found in many industrial fields such as heat exchanger, cooling of electronic devices, solar collectors, and nuclear reactors. Although the most configurations of these enlargement are simple, the study of flow through them acquired increased interest due to presence of associated complex flow events. As reviewing the related studies in this field, it is found that an increased focus given to analyze the flow and thermal characteristics after the expansion region and none studies were reported on adding obstacles to this region. Many studies has been conducted to over the past decades to analyze the flow and heat transfer in sudden expansion channels both in experimental and numerical. Scott *et al.* [1] studied the laminar flow of Newtonian fluid in planar and axisymmetric sudden expansion by solving the continuity and momentum Navier-Stokes equations using the Galerkin finite element formulation. They covered the steady-state flow at Reynolds number up to 200 and expansion ratios of 1.5, 2, 3, and 4. In their study, the effect of Reynolds number and expansion ratio on the re-attachment length, eddy center location, and the relative eddy intensity was investigated. The results showed that the re-attachment length and the eddy center location vary linearly with Reynolds number, but the relative eddy intensity was an exponential function of Reynolds

* Corresponding author; e-mail: khudheyer2004@yahoo.com

number. Tang and Ingham [2] investigated the steady incompressible laminar flow past a sudden expansion assuming two dimensional flow governed by the Navier-Stokes equations. They employed the multi grid method to obtain finite difference solution to the steady Navier-Stokes equations, which were in terms of the vorticity and stream function for Reynolds numbers up to 1000 and uniform inflow. The results showed that the eddy length increased linearly with Reynolds number for both small and large values of expansion ratios. Battaglia *et al.* [3] performed numerical simulations and bifurcation calculations for flow of Reynolds number up to 200 in a 2-D channel with a sudden symmetric expansion. They found the symmetry-breaking bifurcation, representing transition from a symmetric to an asymmetric developing jet. In addition, the critical Reynolds number at the bifurcation point was determined by authors for expansion ratios from 1.5 to 7. The results showed that the critical Reynolds number decreased with increasing expansion ratio. In addition, the results showed that for a fixed expansion ratio, increasing the Reynolds number increased the number of attachment positions for an asymmetric jet. Thiruvengadam *et al.* [4] demonstrated the effects of flow bifurcation on temperature and heat transfer distributions in horizontal duct with plane symmetric sudden expansion. The results obtained by Fluent 6 commercial code. They verified that the maximum Nusselt number that occurs on lower stepped wall is larger than the one that develops on the upper stepped wall and it develops near the sidewall and not at the center of the duct. Baloch *et al.* [5] made numerical investigation for incompressible Newtonian flows through 2- and 3-D expansions. The sudden expansion geometry had a square cross-section. The obtained results show that for Reynolds number up to 10, a significant vortex activity generated by fluid inertia giving re-circulation zone and vortex enhancement. Battaglia and Papadopoulos [6] investigated experimentally and by 2- and 3-D simulations the effect of three dimensionality flows of Reynolds number from 150 to 600 past 2:1 symmetric sudden expansion channel of 6:1 aspect ratio. They showed that comparison of the 2-D simulations with the experiments revealed that the simulations failed to capture completely the total expansion effect on the flow. To do so, requires the definition of an effective expansion ratio (the ratio of the downstream and upstream hydraulic diameters). When 2-D simulations performed using the effective expansion ratio, the new results agreed well with the 3-D simulations and the experiments. Hammed *et al.* [7] studied the laminar flow through an axisymmetric sudden expansion using real-time digital particle image velocimetry. Two dimensional velocity contours obtained for different values of Reynolds number. They verified that the re-attachment length and re-development length downstream of re-attachment were linear functions of Reynolds number. Schreck and Schafer [8] presented numerically the effect of a slight asymmetry in the channel geometry on the flow transition from symmetric to asymmetric in a long channel with a sudden expansion. The results showed that the secondary branch appeared at a certain modified Reynolds number and two addition non-symmetric flow states for Reynolds number greater the critical Reynolds number. Hawa and Rusak [9] investigated the dynamics of 2-D viscous flow in a sudden expansion channel by asymptotic analysis and numerical simulations. The results proved that the critical state at Re_{cr} is a point of exchange of stability for the steady symmetric solutions. Chiang *et al*. [10] investigated the steady bifurcation phenomena for 3-D flows through a plane-symmetric sudden expansion numerically. They showed that the bifurcation was dependent on flow Reynolds number, channel aspect ratio and expansion ratio. Armaly *et al.* [11] reported experimentally the velocity measurements for 3-D laminar separated airflow adjacent to a backward-facing step. The geometry provided an aspect ratio $AR = 8$, and an expansion ratio $ER = 2.02$. They used two-component laser--Doppler velocimeter. The flow measurements covered a Reynolds number range between $98.5 \leq Re \leq 525$. The results showed that the development of reverse and re-circulation flow regions

adjacent to both sidewall and these regions increased in size as Reynolds number increased. Nie and Armaly [12] performed simulations of 3-D laminar forced convection in a plane symmetric sudden expansion. They verified that the maximum Nusselt number was located inside the primary re-circulation flow region and its location did not coincide with swirling flow impingement. Yamaguchi *et al.* [13] obtained experimentally the characteristics of flows in 3-D branching channel geometries. In addition, they gave phenomenological explanations by analyzing the 3-D flow field numerically. It was found from the results of the experiments, which verified by means of numerical simulation, that the defection characteristics were largely dependent upon the net contribution of the swirl component in the expanded channel part. It further revealed that there were different flow distribution characteristics when the distribution outlet pipes were further apart from the center of cylindrical axis in the expanded channel part. Oliveira and Pinho [14] studied the laminar flow of the Newtonian fluid in axisymmetric sudden expansion numerically. They evaluated pressure loss coefficient for a range of Re $\leq$ 225. Also, the values of some overall flow characteristics such the length of re-circulation zone was predicted. Wahba [15] studied the laminar incompressible flow in a symmetric plane sudden expansion numerically, where different iterative solvers on calculation of the bifurcation point were tested. He verified that the type of inflow velocity profile, whether uniform or parabolic has a significant effect on the onset of bifurcation. In the present work, a computational study has been conducted to investigate the dynamic of the flow and heat transfer in an obstacled sudden expansion channel. The obstacles mounted on upper and lower wall of the channel. The obstacles length, obstacles thickness and number of obstacles are investigated for different values of Reynolds number. The consideration of symmetry state is studied. The aim of the present study is to show how the obstacles mounted behind expansion region can affect the dynamics of flow behavior and thermal field.

Model description

The considered physical model is depicted in fig. 1. It represents the upper half of 2-D horizontal channel with a plane symmetric sudden expansion. The upstream height is (h) and the downstream height is (H). The geometry provides a configuration within expansion ratio ($ER = H/h$) equals to 1.5, 1.75, and 2. The downstream length (L_2) equals to 14 times the upstream height is considered where the effect of obstacles is vanished. A fully developed flow is imposed at channel inlet. The insulated obstacles mounted symmetrically on the upper and lower walls of the expansion region and an equal distance (l) between the obstacles is considered. The number of obstacles is varying as 1 and 3. Three obstacle lengths (L_O) equal to 0.1 H, 0.15 H, and 0.2 H, and three obstacles thickness (th) equal to h/24, h/12, and h/6 were studied. Different values of Reynolds number (Re = 50, 100, 150, and 200) were selected taking by consideration the achievement of symmetric flow conditions while the value of Prandtl number was equal to 0.7.

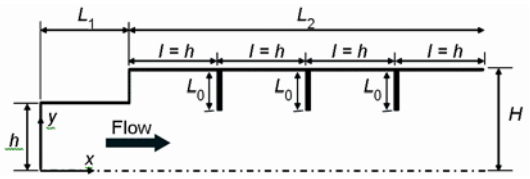

Figure 1. Schematic diagram of the considered problem

Mathematical model

The continuity, Navier-Stokes and energy equations for 2-D steady-state incompressible flow are described below by using the stream function – vorticity formulation.The following assumptions are made:

– fully developed at inlet,
– constant thermo physical properties of the working fluid (air),
– non-slip flow, and
– a constant temperature was imposed at the expansion region walls.

Continuity equation:

$$\frac{\partial u}{\partial x}+\frac{\partial v}{\partial y}=0 \tag{1}$$

Momentum equation in x-direction:

$$\frac{\partial u}{\partial t}+u\frac{\partial u}{\partial x}+v\frac{\partial u}{\partial y}=\upsilon\left(\frac{\partial^2 u}{\partial x^2}+\frac{\partial^2 u}{\partial y^2}\right)-\frac{1}{\rho}\frac{\partial p}{\partial x} \tag{2}$$

Momentum equation in y-direction:

$$\frac{\partial v}{\partial t}+u\frac{\partial v}{\partial x}+v\frac{\partial v}{\partial y}=\upsilon\left(\frac{\partial^2 v}{\partial x^2}+\frac{\partial^2 v}{\partial y^2}\right)-\frac{1}{\rho}\frac{\partial p}{\partial y} \tag{3}$$

Energy equation:

$$\frac{\partial T}{\partial t}+u\frac{\partial T}{\partial x}+v\frac{\partial T}{\partial y}=a\left(\frac{\partial^2 T}{\partial x^2}+\frac{\partial^2 T}{\partial y^2}\right) \tag{4}$$

Differentiate eq. (2) with respect to y and eq. (3) with respect to x and then subtract eq. (2) from eq. (3) and re-arrange the result:

$$\frac{\partial}{\partial t}\left(\frac{\partial v}{\partial x}-\frac{\partial u}{\partial y}\right)+\frac{\partial u}{\partial x}\left(\frac{\partial v}{\partial x}-\frac{\partial u}{\partial y}\right)+\frac{\partial v}{\partial y}\left(\frac{\partial v}{\partial x}-\frac{\partial u}{\partial y}\right)+u\frac{\partial}{\partial x}\left(\frac{\partial v}{\partial x}-\frac{\partial u}{\partial y}\right)+$$
$$+v\frac{\partial}{\partial y}\left(\frac{\partial v}{\partial x}-\frac{\partial u}{\partial y}\right)=\upsilon\left[\frac{\partial^2}{\partial x^2}\left(\frac{\partial v}{\partial x}-\frac{\partial u}{\partial y}\right)+\frac{\partial^2}{\partial y^2}\left(\frac{\partial v}{\partial x}-\frac{\partial u}{\partial y}\right)\right] \tag{5}$$

from the definitions of stream function and vorticity:

$$\mathrm{d}\varphi=u\mathrm{d}y-v\mathrm{d}x \tag{6}$$

$$\Omega=\frac{\partial v}{\partial x}-\frac{\partial u}{\partial y} \tag{7}$$

The governing equations will be:

$$\frac{\partial^2\varphi}{\partial x^2}+\frac{\partial^2\varphi}{\partial y^2}=-\Omega \tag{8}$$

$$\frac{\partial\Omega}{\partial t}+\frac{\partial\varphi}{\partial y}\frac{\partial\Omega}{\partial x}-\frac{\partial\varphi}{\partial x}\frac{\partial\Omega}{\partial y}=\upsilon\left(\frac{\partial^2\Omega}{\partial x^2}+\frac{\partial^2\Omega}{\partial y^2}\right) \tag{9}$$

$$\frac{\partial T}{\partial t}+\frac{\partial\varphi}{\partial y}\frac{\partial T}{\partial x}-\frac{\partial\varphi}{\partial x}\frac{\partial T}{\partial y}=a\left(\frac{\partial^2 T}{\partial x^2}+\frac{\partial^2 T}{\partial y^2}\right) \tag{10}$$

These equations are made dimensionless *via* using the parameters:

$$X=\frac{x}{h},\ Y=\frac{y}{h},\ U=\frac{u}{u_\circ},\ V=\frac{v}{u_\circ},\ \psi=\frac{\varphi}{hu_\circ},\ \tau=\frac{u_\circ t}{h},\ \omega=\frac{\Omega h}{u_\circ},\ \theta=\frac{T-T_\circ}{T_w-T_\circ}$$

Equations (8-10) will become:

$$\frac{\partial^2\psi}{\partial X^2}+\frac{\partial^2\psi}{\partial Y^2}=-\omega \tag{11}$$

$$\frac{\partial\omega}{\partial\tau}+\frac{\partial\psi}{\partial Y}\frac{\partial\omega}{\partial X}-\frac{\partial\psi}{\partial X}\frac{\partial\omega}{\partial Y}=\frac{1}{\mathrm{Re}}\left(\frac{\partial^2\omega}{\partial X^2}+\frac{\partial^2\omega}{\partial Y^2}\right) \tag{12}$$

$$\frac{\partial\theta}{\partial\tau}+\frac{\partial\psi}{\partial Y}\frac{\partial\theta}{\partial X}-\frac{\partial\psi}{\partial X}\frac{\partial\theta}{\partial Y}=\frac{1}{\mathrm{Re\ Pr}}\left(\frac{\partial^2\theta}{\partial X^2}+\frac{\partial^2\theta}{\partial Y^2}\right) \tag{13}$$

Boundary conditions

In order to solve the mathematical model, the boundary conditions were imposed:

– on the upper wall, $\psi=1,\ \omega=-\partial^2\psi/\partial Y^2,\ \theta=1$,
– on the obstacles, $\psi=1,\ \omega=-\partial^2\psi/\partial n^2,\ \partial\theta/\partial n=0$,

where n is a unit normal vector.

On the symmetric line: $\psi=0,\ \partial\theta/\partial Y=0$.

Fully developed conditions are used at inlet: $\partial\varphi/\partial X=0,\ \psi=\psi(Y)$,

where φ represents ψ, Ω, and θ.

At exit, to insure the smooth transition at the flow boundary, the boundary conditions are used:

$$\partial^2\psi/\partial X^2=0;\qquad \partial\omega^2/\partial X^2=0;\qquad \partial^2\theta/\partial X^2=0$$

Grid dependency

To ensure that the hydrodynamic and thermal parameters are not affected by the mesh, different non-uniform grid densities examined for each expansion ratio. For ER = 1.5, the grid densities were (390 × 15), (390 × 30), and (600 × 45). For ER = 1.75, the grid densities (390 × 21), (390 × 35), and (600 × 48). While for ER = 2, the grid densities (390 × 30), (390 × 40), and (600 × 60). It was found that when the grid density increases more than (390 × 30), (390 × 35), and (390 × 40) for ER = 1.5, 1.75, and 2, respectively, there is no significant effect on the trend of results as shown in figs. 2 and 3. Consequently, these grid densities are selected in the present work.

Verification

To verify the present home built computer program, two tests performed with related published results as show in figs. 4-6. As the figures show, the comparison indicated an acceptable agreement. However some discrepancy was pointed due to a degree of used accuracy and type of numerical code.

Symmetry and asymmetry

Figure 7 shows the streamwise velocity contours at Re = 200 and expansion ratio equals to 1.5 (case a), 1.75 (case b), and 2 (case c). It can be seen that at this Reynolds number,

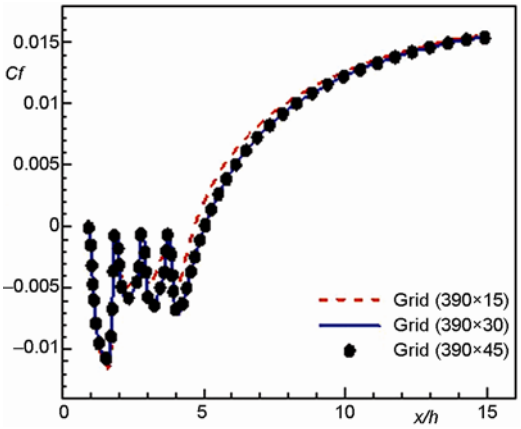

Figure 2. Friction coefficient variation at various grids for Re = 150, *ER* = 1.5, three obstacles, L_o = 0.15 *H*, and *th* = *h*/24

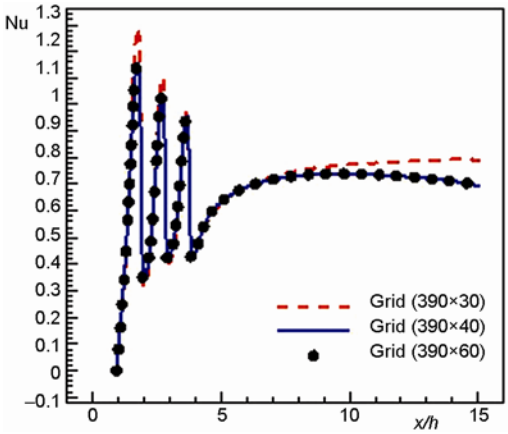

Figure 3. Local Nusselt number variation at various grids for Re = 150, *ER* = 2, three obstacles, L_o = 0.2 *H*, and *th* = *h*/24

two re-circulation zones of equal size mounted symmetrically on upper and lower the center-line of the channel are observed. The streamwise velocity is primarily positive in the direction of flow except for the two re-circulation zones that form immediately downstream of the expanding region where the flow attaches the upper and lower walls. In addition, the figure shows that as the expansion ratio increases, the re-circulation zone becomes larger due to the decreasing in the pressure drop.

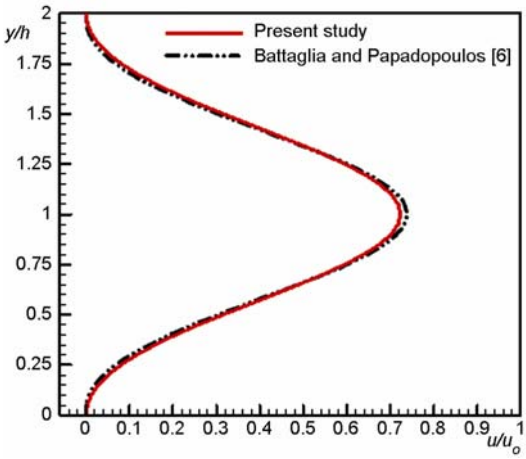

Figure 4. Dimensionless streamwise velocity for *ER* = 2 and *x*/*h* = 4.5, at Re = 171

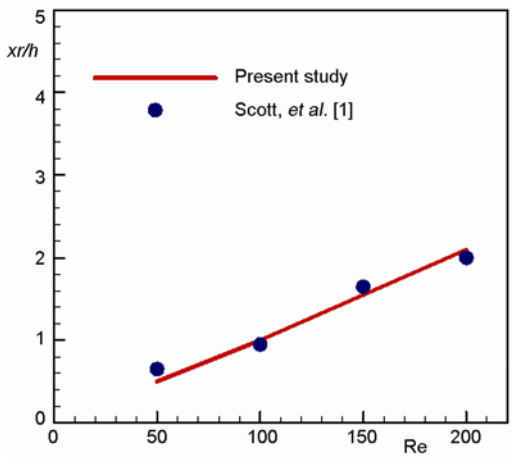

Figure 5. Re-attachment length *vs.* Reynolds number for *ER* = 1.5

The symmetry will disappear as Reynolds number accedes the critical Reynolds number as shown in figs. 8 and 9 where the flow leaves the symmetric state (case a) to asymmetric state (case b) in which different sizes of re-circulation zones are formed along the upper and lower walls. In this study, the symmetry state taken in consideration, which means that the values of studied Reynolds number will not exceed 200 as a general indictor to obtain the symmetry for all the considered expansion ratios.

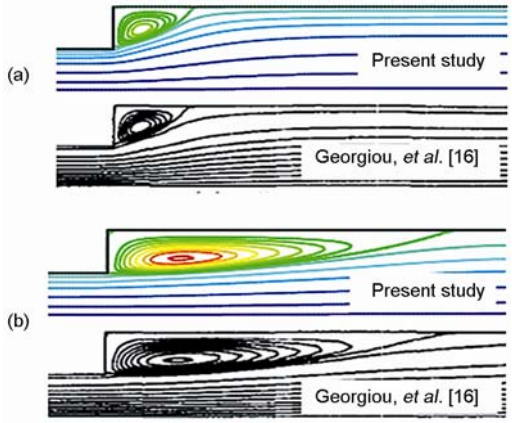

Figure 6. Re-circulation region for 2:1 expansion duct; (a) Re = 10, (b) Re = 50
(for color image see journal web-site)

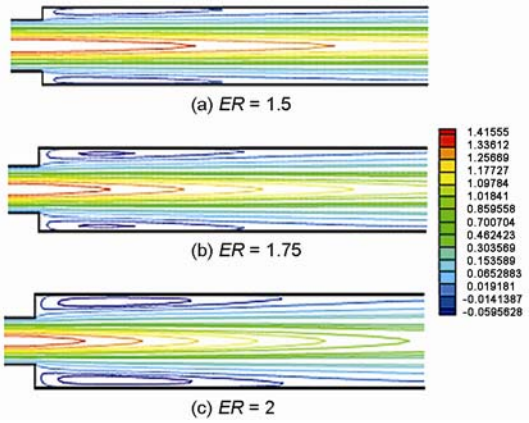

Figure 7. Streamwise velocity distribution with symmetric flow pattern at Re = 200
(for color image see journal web-site)

Results and discussions

Details of obtained results for the 2-D incompressible laminar flow in a sudden expansion obstacled channel are included in this section. Effects of number of obstacles, length of obstacles (L_o), the obstacles thickness (th), and Reynolds number on hydrodynamic and thermal parameters are studied for different expansion ratios.

Effects of the number of obstacles on the hydrodynamic and thermal fields

The effect of number of obstacles on the flow structure at a specified Reynolds number is shown in fig. 10. The stream function contours for the cases of no obstacles, one obstacle, and three obstacles are represented in (a), (b), and (c), respectively. As the obstacles interrupt the development of the boundary layer, the re-circulation zone downstream of the obstacles induced due to the flow separation. Therefore, increasing number of obstacles increases number of re-circulation areas. The figure shows that the re-circulation zone develops to a longe distance by adding one obstacle and it extends longer with four re-circulation zones when adding three obstacles.

Figure 11 shows the effect of adding obstacles on the re-attachment length. It can

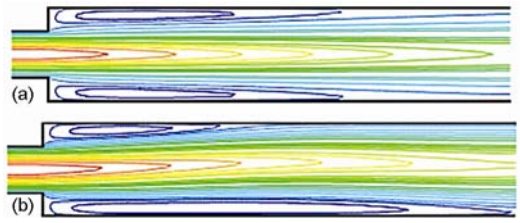

Figure 8. Streamwise velocity contours for *ER* = 2; (a) Re = 200, (b) Re = 230
(for color image see journal web-site)

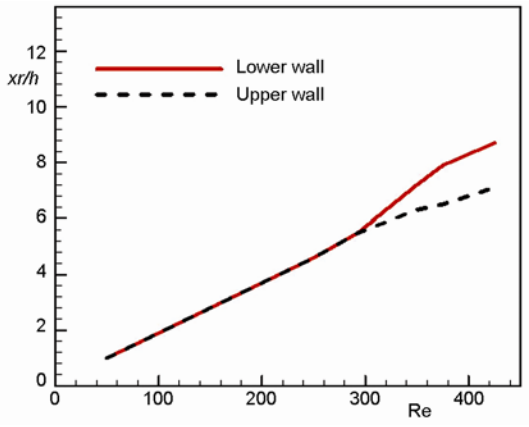

Figure 9. Re-attachment length *vs.* Reynolds number for *ER* = 1.75

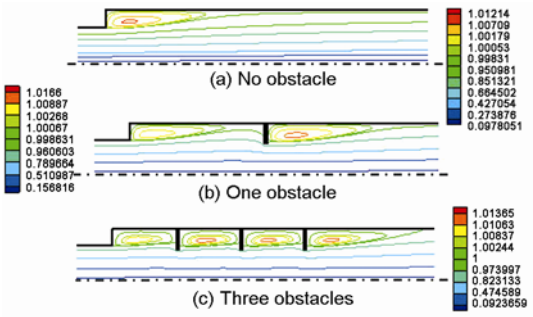

Figure 10. Stream function contours at Re = 100 for *ER* = 1.5, *th* = *h*/24, and L_o = 0.2 *H*
(for color image see journal web-site)

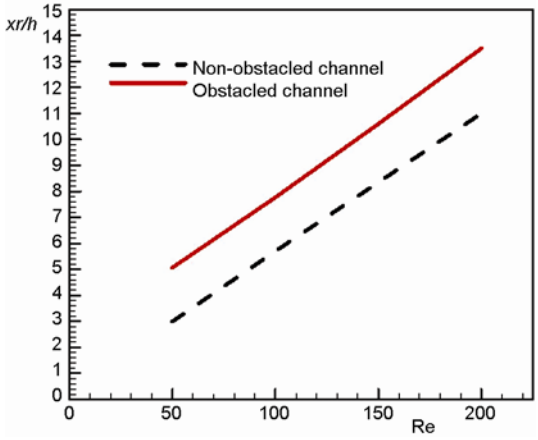

Figure 11. Re-attachment length variation of *ER* = 2 for non-obstacled channel and obstacled channel with one obstacle; *th* = *h*/6 and L_o = 0.2 *H*

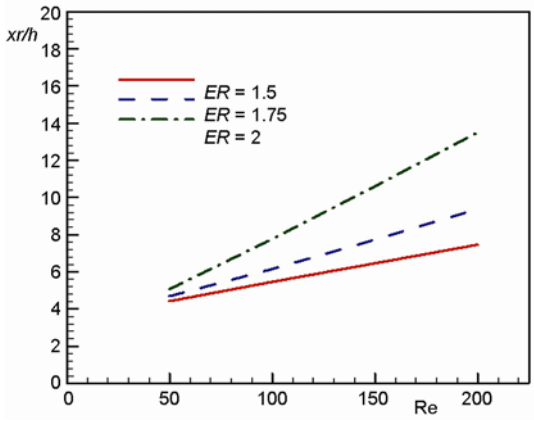

Figure 12. Re-attachment length for obstacled channels with one obstacle; *th* = *h*/6 and L_o = 0.2 *H*

be seen that the re-attachment length is a linear function of the Reynolds number. It also found that if the straight line representing re-attachment length-Reynolds number relationship for non-obstacled channel extends, it would pass through the origin point. This trend is expected considering that the average shear rate at any chosen fixed streamwise distance normalized by the re-attachment length is nearly constant [7]. Adding obstacles will remain the linear function of re-attachment length-Reynolds number relationship but if it extends, it will not pass through the origin. The extended line will shift to pass through a point represents the point of remote separation due to presence of obstacle. Note that the point of separation due to the presence of obstacle coincides with the free edge of the obstacle.

Figure 12 shows the re-attachment length of obstacled channel of different expansion ratios. As in fig. 11, this figure shows that the re-attachment length is a linear function of the Reynolds number. In addition, the re-attachment length increases as the expansion ratio increases because of the increasing in the pressure drop. If these lines in this figure extended, they will pass through the point of remote separation at the free edge of the obstacle.

Figure 13 shows the effect of number of obstacles on the variation of local friction coefficient for *ER* = 2 at Re = 200. It can be seen that the effect of presence of obstacles on the variation in friction coefficient beyond L_2 = 14 times the upstream height is not significant. In addition, it is found that the value of friction factor is fixed at $x/h \geq 61$ which means that the flow is reached to fully developed state.

Figure 14 shows the variation of the average friction coefficient for cases of different number of obstacles. As the number of obstacles increases, the average friction coefficient decreases due to increasing in the re-attachment zone in which the friction coefficient has negative sign.

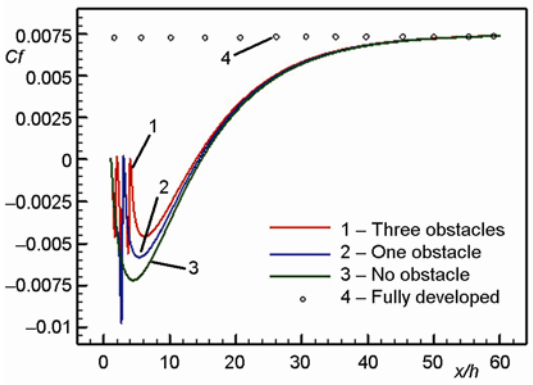

Figure 13. Friction coefficient at upper wall of expansion region at Re = 200 for *ER* = 2, *th* = *h*/12, and L_o = 0.15 *H* *(for color image see journal web-site)*

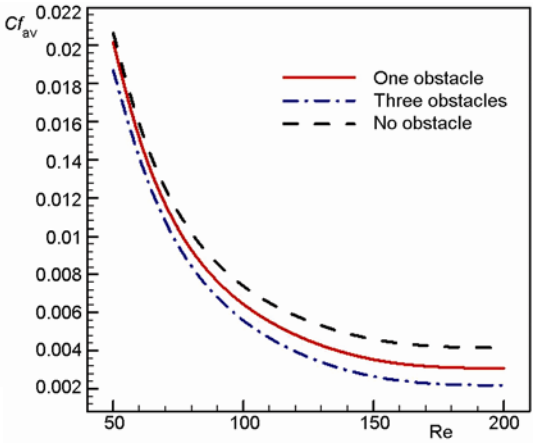

Figure 14. Average friction coefficient for upper wall of expansion region for *ER* = 2, *th* = *h*/6, and L_o = 0.15 *H*

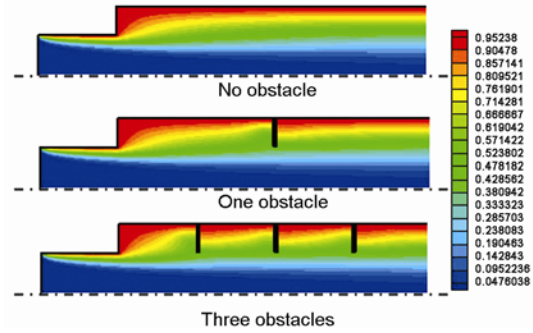

Figure 15. Dimensionless temperature distribution at Re = 150, for *ER* = 1.75, *th* = *h*/24, and L_o = 0.2 *H* *(for color image see journal web-site)*

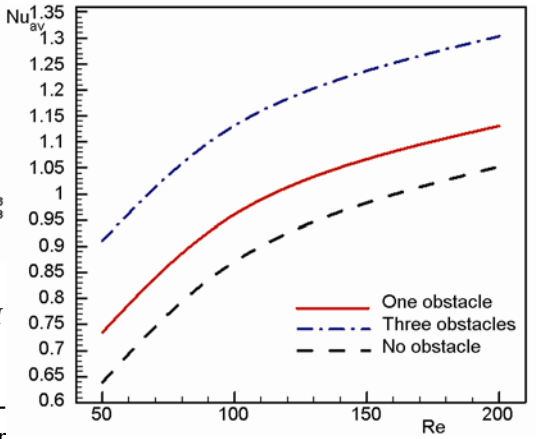

Figure 16. Average Nusselt number at upper wall of expansion region for *ER* = 1.5, *th* = *h*/12, and L_o = 0.2 *H*

Figure 15 represents the contours of dimensionless temperature for different number of obstacles. As the figure shows, the zone of high fluid temperature lie in the obstacled cases (b) and (c). The cause arises to increase re-circulation zones due to presence of obstacles, which increase the mixing and heat losses.

Figure 16 shows the variation of the average Nusselt number *vs.* the Reynolds number for different numbers of the obstacles. As the obstacles number increases, the average Nusselt number increases. The increasing in the average Nusselt number is due to the intense mixing by the induced vortex.

Effects of the length of obstacles on the hydrodynamic and thermal fields

Figure 17 shows the stream function contours for different values of obstacles length L_o. It can be seen that more streamlines will separate due to increase the length of obstacles that leads to increase the area of the re-circulation zone downstream the obstacles because of the increasing in the pressure drop beyond these obstacles.

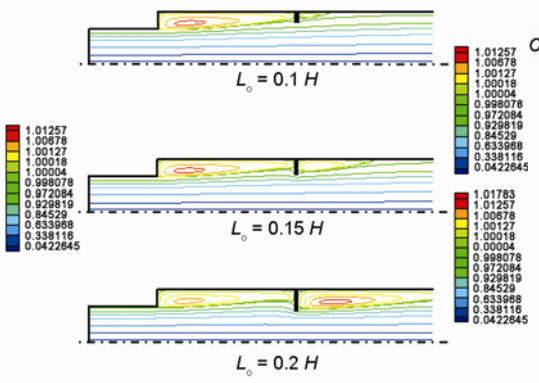

Figure 17. Stream function contours at Re = 150 for *ER* = 1.5, one obstacle case, and *th* = *h*/24 *(for color image see journal web-site)*

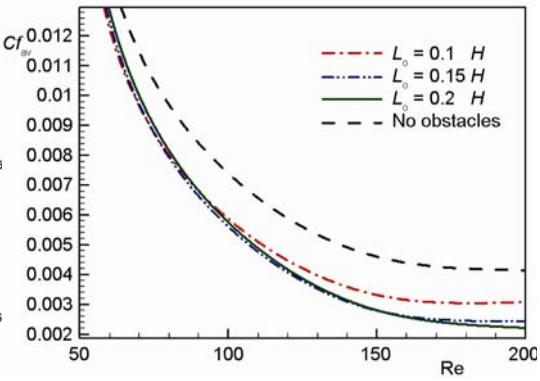

Figure 18. Average friction coefficient at upper wall of expansion region for *ER* = 2, three obstacles case, and *th* = *h*/24

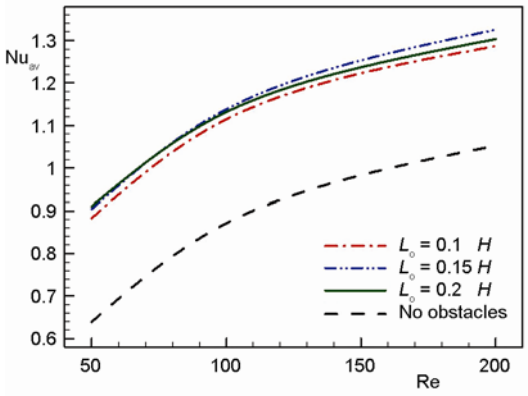

Figure 19. Average Nusselt number at upper wall of expansion region for *ER* = 1.5, three obstacles case, and *th* = *h*/12

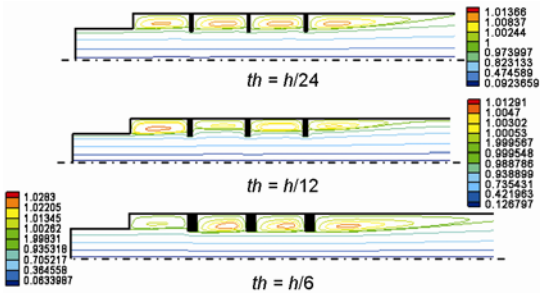

Figure 20. Stream function contours at Re = 150, for *ER* = 1.5, three obstacle case, and L_o = 0.2 *H* *(for color image see journal web-site)*

Figure 18 shows the effect of obstacle length on the variation of the average friction coefficient for different Reynolds number. It can be seen that the value of average friction coefficient for L_o = 0.2 H is lower than those of L_o = 0.15 H, and 0.1 H, due to increase in the separation zone which leads the friction coefficient to remain with negative sign for longer channel length. In addition, this figure shows that the dropping in average friction coefficient and its difference between the compared cases decreased as the Reynolds number increases.

Figure 19 shows the effect of obstacle length L_o on the average Nusselt number. It is found that that as the obstacle length increases, the average Nusselt number increases specially at higher Reynolds number. In addition, there is a coincidence in the average Nusselt numbers for the cases of obstacles length (L_o = 0.15 H and 0.2 H), for 50 ≤ Re ≤ 100.

Effects of the thickness of obstacles on the hydrodynamic and thermal fields

Figure 20 shows the effect of the obstacle thickness (*th*) on stream function contours. It is observed that the length of the re-circulation zone decreases as the obstacles thickness increases from *th* = *h*/24 to *th* = *h*/12, then it increases as the obstacles thickness increases from *th* = *h*/12 to *th* = *h*/6, where the longer re-circulation zone is obtained.

The increasing and decreasing in the friction coefficient with respect to the obstacles thickness is little at higher Reynolds number as seen in fig. 21. In addition, the figure shows that, at lower Reynolds number, the average friction coefficient increases as obstacle thickness increases from *h*/24 to *h*/12, but when obstacle thickness increases from *h*/12 to *h*/6, the friction coefficient decreases following the vorticity behavior according to the obstacle thickness.

The increasing in the Nusselt number for different values of obstacle thickness is seen in fig. 22. It can be observed that there is a significant increasing in the average Nusselt number, as the obstacle thickness increases due to flow mixing enhancement. By increasing the obstacle thickness, the best case of heat transfer augmentation is obtained, which means that the obstacle thickness has the greater effect on the thermal flow parameters when compared with the other obstacles dimensions (its number, length and inclination).

The percentages increase in the average Nusselt number of the obstacled cases at different Reynolds numbers as compared with those of non-obstacled case is in tab. 1.

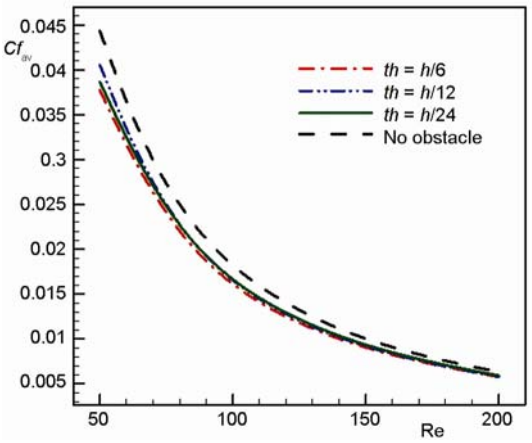

Figure 21. Average friction coefficient at upper wall of expansion region for *ER* = 1.5, three obstacles case, and L_o = 0.15 *H*

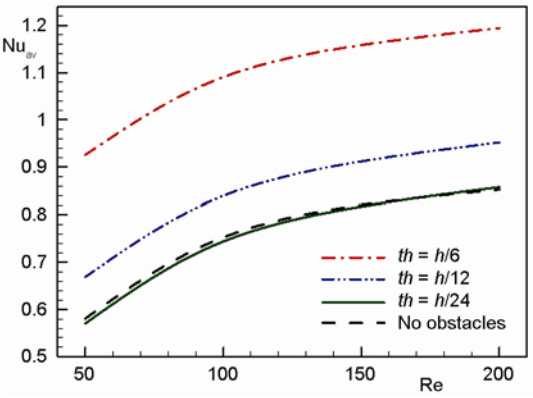

Figure 22. Average Nusselt number at upper wall of expansion region for *ER* = 1.75, one obstacle case, and L_o = 0.1 *H*

Table 1. Percentages increasing in the average Nusselt number for the case of *ER* = 2, three obstacles, L_o = 0.15 *H*, and different Reynolds numbers

th	Re = 50	Re = 100	Re = 150	Re = 200
h/24	–0.161%	1.141%	2.762%	4.490%
h/12	31.673%	26.932%	26.952%	28.343%
h/6	64.535%	59.597%	58.650 %	58.762%

Conclusions

A numerical study of laminar flow in a sudden expansion obstacled channel has been performed. From the obtained results, the following conclusions can reported.

- Adding obstacles just after the channel sudden expansion region, increases the rate of heat transfer by considerable value.
- Increasing number of obstacles increases the rate of heat transfer and decreases drag represented by friction coefficient.
- Increasing obstacle thickness has slight effects on friction drag but it increases Nusselt number significantly at least of 58.65% for *th* = *h*/6.

- Adding obstacles will shift the straight line representing the re-attachment length-Reynolds number relationship to pass through a point represents the point of remote separation.

Nomenclature

Cf – local friction coefficient, [–]
Cf_{av} – average coefficient of friction, [–]
ER – expansion ratio (= H/h), [–]
H – dimensionless downstream channel height, [–]
h – dimensionless upstream channel height, [–]
Nu_{av} – average Nusselt number, [–]
Re – Reynolds number (= Uh/ν), [–]
Pr – Prandtl number (= ν/α), [–]
T – temperature, [°C]
U – dimensionless streamwise velocity, [–]
X, Y – dimensionless co-ordinates, [–]

Greek letters

φ – stream function, [m^2s^{-2}]
ψ – dimensionless stream function, [–]
Ω – vorticity, [s^{-1}]
ω – dimensionless vorticity, [–]
θ – dimensionless temperature, [–]

References

[1] Scott, P. S., *et al*., A Finite Element Analysis of Laminar Flows through Planar and Axisymmetric Abrupt Expansions, *Computers and Fluids, 14* (1986), 4, pp. 423-432
[2] Tang, T., Ingham, D. B., Multigrid Solutions of Steady Two-Dimensional Flow past a Cascade of Sudden Expansions, *Computers and Fluids, 21* (1992), 4, pp. 647-660
[3] Battaglia, F., *et al.*, *Bifurcation of Low Reynolds Number Flows in Symmetric Channels*, American Institute of Aeronautics and Astronautics, 1996
[4] Thiruvengadam, M., *et al*., Bifurcated Three-Dimensional Forced Convection in Plane Symmetric Sudden Expansion, *International Journal of Heat and Mass Transfer, 48* (2005), 15, 3128–3139
[5] Baloch, A., *et al*., On Two and Three Dimensional Expansion Flows, *Computers and Fluids, 24*, (1995), 8, pp. 863-882
[6] Battaglia, F., Papadopoulos, G., Bifurcation Characteristics of Flows in Rectangular Sudden Expansion Channels, *Journal of Fluids Engineering, 128* (2006), 4 pp. 671-679
[7] Hammad, K. J., *et al*., A PIV Study of the Laminar Axisymmetric Sudden Expansion, *Flow Experiments in Fluids 26* (1999), 3, 266-272
[8] Schreck, E., Schafer, M., Numerical Study of Bifurcation in Three Dimensional Sudden Channel Expansions, *Computers and Fluids, 29* (2000), 5, pp. 583-593
[9] Hawa, T., Rusak, Z., The Dynamics of a Laminar Flow in a Symmetric Channel with a Sudden Expansion, *J. Fluid Mech., 436* (2001), June, pp. 283-320
[10] Chiang, T. P., *et al*., Spanwise Bifurcation in Plane Symmetric Sudden Expansion Flows, *Physical Review E., 65* (2001), 016306
[11] Armly, B. F., *et al*., Measurements in Three Dimensional Laminar Separated Flow, *International Journal of Heat and Mass Transfer, 46* (2006), 19, pp. 3573-3582
[12] Nie, J. H., Armaly, B. F., Three-Dimensional Forced Convection in Plane Symmetric Sudden Expansion, *Journal of Heat Transfer, 126* (2004), 5, pp. 836-839
[13] Yamaguchi, H., *et al*., Basic Flow Characteristics in Three-Dimensional Branching Channel with Sudden Expansion, *European Journal of Mechanics B/Fluids 25* (2006), 6, pp. 909-922
[14] Oliveira, P. J., Pinho, F. T., Pressure Drop Coefficient of Laminar Newtonian Flow in Axisymmetric Sudden Expansions, *Int. J. Heat and Fluid Flow, 18* (1977), 5, pp. 518-529
[15] Wahba, E. M., Iterative Solvers and Inflow Boundary Conditions for Plane Sudden Expansion Flows, *Applied Mathematical Modeling, 31* (2007), 11, pp. 2553-2563
[16] Georgiou, G. C., *et al.*, Singular Finite Elements for the Problems Sudden-Expansion and the Die-Swell, *International Journal for Numerical Methods in Fluids, 10* (1990), 4, pp. 357-372

Paper submitted: October 29, 2012
Paper revised: July 10, 2013
Paper accepted: July 13, 2013